

Detection of Growth-Restricted Fetuses using a Patient-Specific Model

O. Barnea, O. Luria, and J. Bar

Abstract— Fetal growth restriction (FGR) is one of the major contributors to adverse perinatal outcome. The purpose of this work was to extend the use of Ultrasound Doppler measurements and allow early and accurate detection of FGR. To this end, a mathematical model was developed to represent the major fetal hemodynamic mechanisms involved. Based on model parameters' values, the forward model predicted flow waveforms at the locations where Doppler measurements are routinely performed. Blood velocity waveforms measured in 20 FGR and 20 normal fetuses were used as inputs to an inverse model solution to obtain the parameters' values of the specific fetus. Model predictions indicated significant changes in the circulation of FGR fetuses compared to normal fetuses. Estimated cardiac output was significantly lower in the FGR group compared to the control group ($330 \pm 52 \text{ ml min}^{-1} \text{ Kg}^{-1}$ compared to $396 \pm 52 \text{ ml min}^{-1} \text{ Kg}^{-1}$, $P < 0.001$). Also, estimated cardiac output distribution towards the placenta was lower for the FGR group ($145 \pm 49 \text{ ml min}^{-1} \text{ Kg}^{-1}$ compared to $181 \pm 31 \text{ ml min}^{-1} \text{ Kg}^{-1}$, $P < 0.01$). In the FGR group the model indicated also significant increase in estimated cardiac output distribution towards the brain ($9.6 \pm 0.7\%$, compared to $8.0 \pm 1.6\%$, $P < 0.01$) and in the degree of blood shunted by the ductus venosus ($60.6 \pm 17.7\%$, compared to $39.7 \pm 14.8\%$, $P < 0.01$), indicating severe brain-sparing state in these fetuses. We conclude that patient-specific mathematical modeling is a promising direction for personalizing and optimizing the treatment options in pregnancies complicated by fetal growth-restriction.

I. INTRODUCTION

Fetal growth restriction (FGR) is one of the major challenges in antenatal care and an important determinant for perinatal mortality and morbidity [1, 2]. FGR fetuses fail to reach their growth potential and remain below the 10th percentile of the normal growth curve. FGR may result from genetic disorders, infection or uteroplacental insufficiency. In growth-restricted fetuses, abnormal placentation leads to placental insufficiency, vascular-compromised blood supply and reduced oxygenation. These pathological conditions may evolve to hypoxia and acidemia, resulting in adverse pregnancy outcome.

When FGR is developed, the fetus adapts by progressively triggering compensatory mechanisms. These mechanisms include an increase in the fractional oxygen extraction and redistribution of the cardiac output towards the brain, heart and adrenals [3]. These compensatory actions are referred to as 'brain-sparing effect', as this mechanism is aimed at maintaining cerebral oxygenation at the expense of non-vital organs.

The cardiovascular response of the brain-sparing effect is well documented in both human and animal studies [3-5]. This response includes an increase in placental and peripheral resistance to blood flow with concomitant decrease in the cerebral vascular resistance. This twofold mechanism leads to an increase in the right ventricular afterload [6,7] and a decrease in the left ventricular afterload [7,8]. Due to the parallel structure of the fetal circulation, these changes result in preferential distribution of the cardiac output towards the left ventricle, resulting in an increase in the cerebral and coronary blood flows [9]. On the venous side, the shunting of the umbilical venous blood through the ductus venosus increases in response to the intrauterine hypoxia. This results in increased oxygenated blood flow toward the left atrium. Thus, the overall impact of the brain-sparing effect is an improved distribution of oxygenated blood towards the heart and brain.

In mild placental insufficiency, the brain-sparing effect successfully maintains cerebral oxygenation. As the hypoxic state prolongs, a nadir in the cerebral vasodilatation is observed while the placental resistance to blood flow continues to increase. In severe FGR, the brain-sparing effect ultimately collapses, resulting in the de-compensatory stage of FGR [4,5]. The prevention of hypoxic brain injury in this stage remains a major clinical challenge in the management of FGR pregnancies.

As a result of the placental insufficiency and development of the brain-sparing effect, significant changes in the morphology of the flow velocity waveform (FVW) in the large vessels of the fetal circulation are observed. Increased pulsatility of the umbilical artery is one of the most common signs of placental insufficiency. Absent or reversed end-diastolic flow in the umbilical arteries is associated with an increased rate of perinatal mortality [10]. As a result of cerebral vasodilation, the pulsatility of the middle cerebral artery FVW reduces, indicating the triggering of the brain-sparing effect. As a result, the ratio between UA PI (umbilical artery pulse index) to MCA PI (middle cerebral artery) increases. The peaks ratio (E/A) in the waveforms of the mitral and tricuspid valves is increased as a consequence of the high pressure in the ventricles, due to increased afterload. As the degree of fetal hypoxemia and acidemia increases, Doppler changes are observed also in the fetal veins. In the ductus venosus, blood flow velocity during the atrial contraction ('a' wave) reduces and may even become negative in severe cases of FGR, indicating a reversal of blood flow. Umbilical vein pulsation can also develop in FGR fetuses.

Extensive effort has been focused at the development of diagnostic techniques for estimating fetal well-being. In the clinical practice, accurate estimation of the hemodynamic status of the fetus is especially important when monitoring pregnancies complicated by fetal growth restriction, where the fetus is subjected to intrauterine hypoxia. Currently, the principal tools for the evaluation of the hemodynamic status of FGR fetuses are Doppler velocimetry, combined with functional testing such as the biophysical profile and non-stress test. Doppler indices reflect the degree of fetal compromise, but provide only a qualitative assessment of its hemodynamic status. Doppler indices also suffer from significant variability between fetuses, expressed by the large variance in the reference curves for normal Doppler indices. Therefore, those charts have limited diagnostic value regarding the specific fetus examined.

Given that the measurement of hemodynamic quantities such as blood pressure and flow is not possible in-utero, research into fetal hemodynamics is often based on estimations of these parameters which are based on mathematical modeling of the fetal circulation. Those models simulate fetal circulation in normal and pathological conditions and estimate physiological quantities of clinical interest.

The purpose of this work was to develop a method that will extract more information from FVWs. A mathematical model of the fetal circulation was developed. The forward model generated blood FVWs for a set of cardiovascular parameter values. Same waveforms that were measure in fetuses were used in an inverse solution of the model that calculated the set of cardiovascular parameter values that will generate the measured waveforms. This allowed us to estimate parameters' values that cannot be measured directly and help in the detection of growth restriction in fetuses.

II. METHODS

A mathematical model was developed based on the structure of fetal circulation in singleton pregnancies, while emphasizing the most significant components: the fetal heart, brain, lungs, systemic circulation and the fetal part in placental circulation. A diagram of the model is illustrated in Figure 1. In this multi-element model, blood from the left ventricle (LV) flows towards the aorta, where it is divided between the carotid arteries towards the brain (BR), heart, upper body (UB) and the descending aorta (AO). Most of the blood from the right ventricle (RV) bypasses the lungs through the ductus arteriosus (DA), which connects the pulmonary trunk to the descending portion of the aortic arch. Blood carried by the descending aorta is divided between the branches of the aorta supplying the organs of the lower regions of the torso (LB) and the umbilical arteries supplying blood to the placenta (PLA). Some of the oxygenated blood from the placenta is routed around the liver by the ductus venosus (DV) towards the left atrium and ultimately perfuses into the fetal brain. The remaining blood enters the liver and constitutes the hepatic blood flow (HE). Blood from the internal organs is drained by the inferior vena cava (IVC) and enters the right atrium (RA). Blood from the brain and upper extremities is drained by the superior vena cava (SVC) and enters the RA. Thus, the fetal cerebral oxygen blood flow depends upon placental blood flow, the volume of blood shunted by the DV and cerebral blood flow.

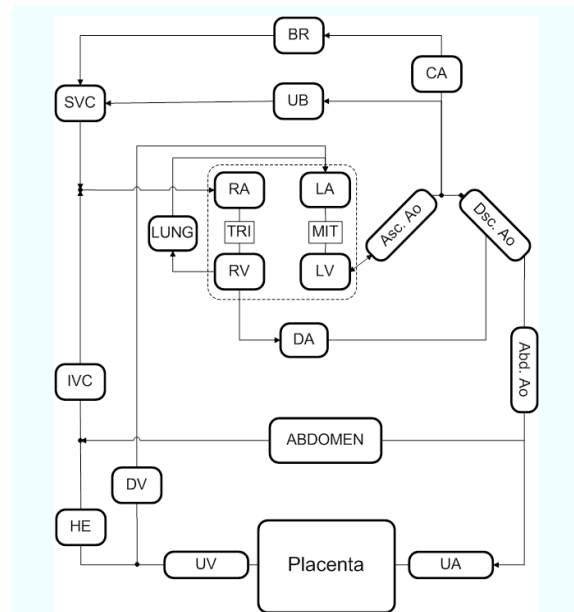


Figure 1. Structure of the hemodynamic model

The contracting chambers were based on the well-known Suga-Sagawa "varying elastance" model and the circulation was modeled to reflect the viscous and inertial forces, represented by a resistor (R_i) and an inductor (L_i), respectively, as well as the elasticity of the blood vessels, represented by a capacitor (C_i) [11].

The model was designed to represent the fetal circulation between 21 to 40 weeks of gestation. During that period, fetal weight increases from 400 grams to 3,400 gram [12]. Scaling of model elements, such as the volume of fetal heart chambers, resistance of blood vessels, blood vessel inertance and the compliance of internal organs was based on the results presented by Dawson [13] regarding the scaling of vascular networks in mammals.

The forward model of fetal circulation is complex and includes a large number of parameters (total of 48 parameters that characterize the dynamic properties of the main elements in the model). An efficient solution of the inverse problem requires a reduction in the number of model parameters. To achieve an effective compromise between model complexity and usefulness, a minimal set of parameters (factors) was defined to describe the relevant aspects of the compensatory mechanisms observed in FGR. Three major mechanisms were chosen based on clinical significance: reduction in placental blood flow or decreased vessel radius, cerebral vasodilation (increased radius) and the increase in the percentage of blood shunted by the ductus venosus (also change in vessel radius):

$$F = [F^{PLA}, F^{BR}, F^{DV}] \quad (1)$$

where F^{PLA} is a placental vasodilation factor; F^{BR} is cerebral vasodilation factor and F^{DV} is the ductus venosus shunt flow factor. Each factor affects the resistance, compliance and inertance of specific model segments. An increase in each factor corresponds to a decrease in the resistance and inertance and an increase in the compliance of the model segment, in both arterial and venous side of each vascular bed, according to Eq. 2:

$$R_i = \frac{(F^i)^{n_R}}{R_{i,0}^S} \quad L_i = \frac{L_{i,0}^S}{(F^i)^{n_L}} \quad C_i = C_{i,0}^S \times (F^i)^{n_C} \quad (2)$$

where R_i , L_i and C_i are resistance, inertance and compliance, respectively; i represents *PLA*, *BR* or *DV* for the placental, cerebral or ductus venosus, respectively, and n is a power exponent. $R_{i,0}^S$, $L_{i,0}^S$, and $C_{i,0}^S$ are the originally preset values of each segment. They are inter-related since they all depend on the radius of the segment: $R_{i,0} = f\left(\frac{1}{r^4}\right)$; $L_{i,0} = g\left(\frac{1}{r^2}\right)$; $C_{i,0} = h(r^3)$.

The forward model, was used to generate baseline waveforms similar to those measured in healthy normal fetuses. Then, the inverse solution was developed to yield parameters' values that will generate the waveforms measured in FGR fetuses based on measured velocities.

The inverse solution started with generating a kernel model that describes a normal fetus of the same weight with normal FVWs. To estimate model parameters, we used nonlinear optimization to minimize the residual between the computed and measured (noted by superscript \wedge) flow waveforms. To achieve that aim, the waveforms vectors v and \hat{v} were defined (Eq 3), spanning all the measured FVWs and calculated flow waveforms for the umbilical artery, middle cerebral artery, ductus venosus, tricuspid valve and mitral valve, respectively. Since the measured Doppler signals depend upon the insonation angle, signals were first normalized in amplitude. To cancel the effects of signal amplitude on the parameter estimation process, calculated flow waveforms were normalized in the same way.

$$\begin{aligned} v &= \left[v^{UA}, v^{MCA}, v^{DV}, v^{TRI}, v^{MIT} \right]^T \\ \hat{v} &= \left[\hat{v}^{UA}, \hat{v}^{MCA}, \hat{v}^{DV}, \hat{v}^{TRI}, \hat{v}^{MIT} \right]^T \end{aligned} \quad (3)$$

The residual vector \hat{R} , which describes the averaged error between the calculated and measured waveforms over four fetal heart cycles, was defined as follows:

$$\hat{R} = \left[\begin{array}{c} v^{UA} - \hat{v}^{UA}, v^{MCA} - \hat{v}^{MCA}, v^{DV} - \hat{v}^{DV}, \\ v^{TRI} - \hat{v}^{TRI}, v^{MIT} - \hat{v}^{MIT} \end{array} \right]^T \quad (4)$$

Consequently, the cost-function J was defined as an averaged mean squared error (MSE) between the velocity and flow waveforms:

$$J = \hat{R}^T \hat{R} = \frac{1}{N} \sum \left[\left| v^{UA} - \hat{v}^{UA} \right|^2 + \left| v^{MCA} - \hat{v}^{MCA} \right|^2 + \left| v^{DV} - \hat{v}^{DV} \right|^2 + \left| v^{TRI} - \hat{v}^{TRI} \right|^2 + \left| v^{MIT} - \hat{v}^{MIT} \right|^2 \right] \quad (5)$$

Thus, the estimation problem was presented as the search for the parameter set F which minimizes J in the least-squares sense. The search was performed iteratively, while each element of F was optimized individually. The three elements of parameter vector F were estimated in the following order, from the arterial side to the venous side of the fetal circulation: placental vasodilation factor F^{PLA} , cerebral vasodilation factor F^{BR} , following by the ductus venosus shunt flow factor F^{DV} . This order of parameters was designed to favor the arterial parameters over the venous-related parameters that are considered too have a more passive role in determining the

shape of the flow-velocity waveforms. In each iteration, parameters were set with values that minimized the mean squared error between the model waveforms and specific FVWs that were measured by the Doppler ultrasound (i.e., in the umbilical artery, middle cerebral artery and ductus venosus, respectively). Following the change in each parameter, all relevant model parameters were updated. Then, the entire model was simulated until a steady-state conditions were established in all its generated flow waveforms and cardiac chambers pressure-volume loops. This process continued until the mean squared error between the model waveforms and measured FVWs was less than a predefined threshold value. The values used in the model were restricted to their physiological range.

The model was tested on 42 women (20 normal pregnancies and 22 pregnancies complicated by fetal growth restriction). Maternal age and percentage of primiparas were similar in the study and control groups. Gestational age at delivery, birth weight and birth weight percentile were significantly lower in the FGR group, as expected from the study design. A higher rate of adverse fetal/neonatal outcome was observed in the FGR group; two intrauterine fetal deaths (9%) occurred, three neonates (14%) developed respiratory complications, yielding overall, five neonates (23%) with composite adverse outcomes, compared with none in the control group ($P=0.03$). The number of hospitalization days in the neonatal intensive care unit was also significantly higher in the FGR group compared with the control group ($P=0.01$), as was to be expected.

III. RESULTS

Four hemodynamic indices were defined as estimates of fetal hemodynamic status based on FGR pathologies:

(a) *Combined cardiac output normalized to fetal weight* (in $\text{mL min}^{-1} \text{Kg}^{-1}$), calculated as the product of the combined stroke volume and fetal heart rate, divided by fetal weight. This index indicates the ability of the fetal heart to cope with an increase in cardiac preload caused by placental insufficiency; (b) *Placental blood flow normalized to fetal weight* (in $\text{mL min}^{-1} \text{Kg}^{-1}$). This index reflects the extent of placental insufficiency, expressed as an increase in placental resistance to blood flow; (c) *Cardiac output distribution towards the brain* (as a percentage of total cardiac output). This value reflects the twofold effect of increased placental resistance to blood flow and the triggering of cerebral vasodilation. Both mechanisms have a direct effect on cerebral blood flow; (d) *Degree of blood shunted by the ductus venosus* (as a percentage of umbilical vein blood flow). This index reflects the triggering of the compensatory mechanisms deployed to maintain cerebral perfusion. An increase in the ratio of blood shunted by the ductus venosus causes reduced hepatic oxygenation and can indicate the development of intrauterine hypoxia.

Figure 2 shows the results of the patient specific hemodynamic indices obtained from the model for all subjects. Cardiac output (inset A), placental blood flow (inset B), cerebral blood flow (inset C) and % of cerebral cardiac output (inset D) are shown. Results refer to the control group ($N=20$), the FGR group ($N=22$), and the subgroup of FGR fetuses, which suffered from an adverse outcome ($N=5$).

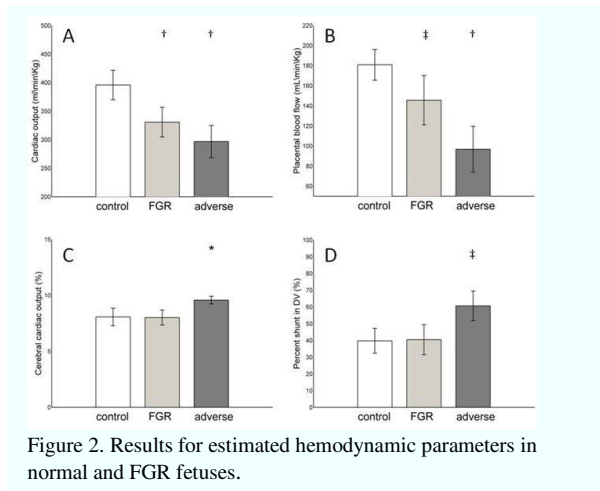


Figure 2. Results for estimated hemodynamic parameters in normal and FGR fetuses.

Cardiac output was significantly lower in the FGR group when compared with the control group ($330 \pm 52 \text{ ml min}^{-1} \text{ Kg}^{-1}$ and $396 \pm 52 \text{ ml min}^{-1} \text{ Kg}^{-1}$, $P < 0.001$, respectively). Furthermore, cardiac output distribution towards the placenta was lower in the FGR group ($145 \pm 49 \text{ ml min}^{-1} \text{ Kg}^{-1}$ and $181 \pm 31 \text{ ml min}^{-1} \text{ Kg}^{-1}$, $P < 0.01$, respectively). In FGR fetuses with an adverse outcome, both indices were even lower ($297 \pm 56 \text{ ml min}^{-1} \text{ Kg}^{-1}$, $P < 0.001$ and $97 \pm 46 \%$, $P < 0.001$, respectively). In the adverse outcome group the model also indicated a significant increase in cardiac output distribution towards the brain ($9.6 \pm 0.7 \%$, and $8.0 \pm 1.6 \%$, $P < 0.01$, respectively) and in the percentage of blood shunted by the ductus venosus ($60.6 \pm 17.7 \%$, and $39.7 \pm 14.8 \%$, $P < 0.01$, respectively), indicating a severe brain sparing state.

Table 1 summarizes the deviance (statistical quality of fit), sensitivity, specificity and area under ROC curve (AUROC) for subsets of clinical Doppler tests and patient specific hemodynamic indices in correctly detecting FGR.

Table 1.

| Signal Subset | Deviance | Sensitivity (%) | Specificity (%) | AUROC |
|--------------------------------|----------|-----------------|-----------------|-------|
| Subset A | 54.2 | 75 | 48 | 0.66 |
| Subset B | 31.4 | 65 | 78 | 0.75 |
| Hemodynamic Indices | 38.2 | 80 | 74 | 0.85 |
| Subset A + Hemodynamic Indices | 35.9 | 70 | 87 | 0.86 |
| Subset B + Hemodynamic Indices | 18.3 | 75 | 91 | 0.83 |

Subset A: {UA, MCA}; subset B: {UA, MCA, DV PVIV, MIT, TRI}, hemodynamic indices: {CO, placental blood flow, % shunt in DV, % of cerebral blood flow, P^{PLA} , P^{BR} , P^{DV} }.

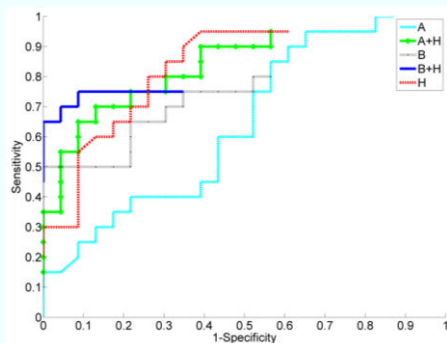


Figure 3. Receiver operating characteristic for the signal subsets shown in Table 1.

IV. DISCUSSION

A methodology for patient specific modelling was presented. It was applied for the estimation of cardiovascular parameters in fetal circulation and was validated in 42 fetuses.

The mathematical model was shown to generate accurate descriptions of fetal flow waveforms throughout the gestational period for both normal and FGR fetuses. In FGR fetuses, the model predicted cardiac output and placental blood flow significantly below normal. Fetuses showing adverse outcome were identified as having a significant increase in the distribution of cardiac output towards the brain and in the percentage of blood shunted by the ductus venosus, indicating the development of a brain sparing effect. Figure 3 indicates that the addition patient specific hemodynamic indices to a subset of Doppler data is more sensitive than conventional Doppler indices alone for the identification of FGR pregnancies.

V. CONCLUSIONS

The use of the model was shown to result in 80% sensitivity and add significant information beyond the traditional analysis of the Doppler waveforms. The diagnostic results for patient specific hemodynamic indices combined with the Doppler indices reached 75% sensitivity and 91% specificity, with an AUROC of 0.83.

REFERENCES

- Baschat AA. Fetal growth restriction - from observation to intervention. *J Perinat Med.* 2010;38:239-46.
- Kramer MS, Olivier M, McLean FH, Willis DM, Usher RH. Impact of Intrauterine Growth Retardation and Body Proportionality on Fetal and Neonatal Outcome. *Pediatrics.* 1990;86:707-13.
- Baschat DAA. Fetal responses to placental insufficiency: an update. *BJOG: An International Journal of Obstetrics & Gynaecology.* 2004;111:1031-41.
- Lerner JP. Fetal growth and well-being. *Obstet Gynecol Clin North Am.* 2004;31:159-76.
- Botsis D, Vrachnis N, Christodoulakos G. Doppler assessment of the intrauterine growth-restricted fetus. *Ann N Y Acad Sci.* 2006;1092:297-303.
- Griffin D BK, Masini L, Diaz-Recasens J, Pearce JM, Willson K, Campbell S. Doppler blood flow waveforms in the descending thoracic aorta of the human fetus. *Br J Obstet Gynaecol.* 1984;91:997-1006.
- Wladimiroff JW, Tonge HM, Stewart PA. Doppler ultrasound assessment of cerebral blood flow in the human fetus. *Br J Obstet Gynaecol.* 1986;93:471-5.
- Arbeille P, Maulik D, Fignon A, Stale H, Berson M, Bodard S, Locatelli A. Assessment of the fetal PO2 changes by cerebral and umbilical Doppler on lamb fetuses during acute hypoxia. *Ultrasound Med Biol.* 1995;21:861-70.
- Baschat AA, Gembruch U, Gortner L, Reiss I, Weiner CP, Harman CR. Coronary artery blood flow visualization signifies hemodynamic deterioration in growth-restricted fetuses. *Ultrasound Obstet Gynecol.* 2000;16:425-31.
- Alfirevic Z, Neilson JP. Doppler ultrasonography in high-risk pregnancies: Systematic review with meta-analysis. *American journal of obstetrics and gynecology.* 1995;172:1379-87.
- Barnea O, Moore T, Jaron D. Computer simulation of the mechanically-assisted failing canine circulation. *Annals of Biomedical Engineering.* 1990;18:263-83.
- Gallivan S, Robson SC, Chang TC, Vaughan J, Spencer JAD. An investigation of fetal growth using serial ultrasound data. *Ultrasound in Obstetrics and Gynecology.* 1993;3:109-14.
- Dawson TH. Modeling of vascular networks. *J Exp Biol.* 2005;208:1687-94.